Check for updates



www.chembiochem.org

Spontaneous Fusion of Aqueous Two-Phase Droplets: Effect of Coexisting Phospholipids on Stability

Mayu Shono,* Maika Inoue, Daigo Yamamoto, Miho Yanagisawa,* Kenichi Yoshikawa, and Akihisa Shioi*

The stability of aqueous two-phase system (ATPS) droplets is a key requirement for extending their utility beyond conventional applications, particularly as minimal models of biological cells and reaction compartments. However, the mechanisms by which their dynamic process in droplet size growth remain poorly understood. In this study, lecithin is demonstrated to effectively stabilize ATPS droplets by modulating two fundamental processes that determine their size evolution: 1) approaching migration driven by thermal motion and inter-droplet attraction and 2) the coalescence initiation time, defined as the delay between first contact and the onset of merging. Using dextran-rich droplets dispersed

in a polyethylene glycol phase, significant suppression of both processes is shown that occurs only when lecithin concentrations exceed its critical micelle concentration. The findings indicate that lecithin coats droplet surfaces spontaneously to form a membrane-like layer, thereby reducing inter-droplet attraction and strongly inhibiting coalescence. This stabilization strategy offers a simple yet powerful means to control droplet dynamics, thereby opening up new possibilities for engineering ATPS droplets as versatile platforms for biochemical reactions and synthetic cell research.

1. Introduction

Aqueous two-phase systems (ATPSs), formed from mixtures of water-soluble polymers, have been extensively studied as versatile platforms for the extraction, separation, and purification of biomolecules and cells.^[1] More recently, ATPS droplets have gained growing attention in synthetic biology and biophysics as simplified models of cells. Their compartmentalized microenvironments mimic the crowded interior of biological cells by spontaneously encapsulating macromolecules such as DNA and F-actin.^[2-6] Moreover, phospholipid adsorption at droplet surfaces can generate cellular membrane-like structures, further enhancing their resemblance to biological cells.^[2,7]

A critical requirement for such applications is droplet stability. However, ATPS droplets tend to coalesce and to grow larger by decreasing the instability due to the interfacial energy, leading to

macroscopic phase separation. In typical polyethylene glycol (PEG) and dextran (DEX) systems, micro droplets exhibit the coarsening to macroscopic phase separation with the time scale of minutes to tens of minutes. Accordingly, considerable effort has been devoted to developing strategies to stabilize ATPS droplets.[8-13] It is reported that adsorption and layering of phospholipids and other lipids at droplet interfaces can reduce droplet growth rates. [6,8,12,14-22] Rowland and Keating demonstrated that the adsorption of small unilamellar vesicles (SUVs) composed of zwitterionic phosphatidylcholine, anionic phosphatidylglycerol, and PEGylated phospholipids can effectively stabilize various ATPS droplets within the PEG aqueous phase.[8] Notably, their findings revealed that even SUVs prepared via simple vortex mixing, as opposed to conventional extrusion methods, were sufficient for achieving functional stabilization, thereby simplifying the preparation process. The lipid-stabilized ATPS droplets

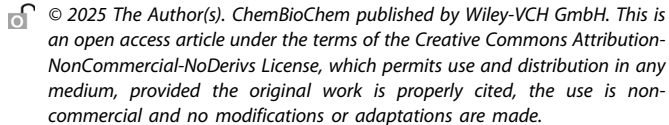
M. Shono, M. Yanagisawa Komaba Institute for Science Graduate School of Arts and Sciences The University of Tokyo Komaba 3-8-1, Meguro, Tokyo 153-8902, Japan E-mail: mshono@g.ecc.u-tokyo.ac.jp myanagisawa@g.ecc.u-tokyo.ac.jp

M. Inoue, D. Yamamoto, A. Shioi
Department of Chemical Engineering and Materials Science
Doshisha University
Kyoto 610-0321, Japan
E-mail: ashioi@mail.doshisha.ac.jp

M. Yanagisawa Center for Complex Systems Biology Universal Biology Institute The University of Tokyo Komaba 3-8-1, Meguro, Tokyo 153-8902, Japan M. Yanagisawa Graduate School of Science Department of physics The University of Tokyo Hongo 7-3-1, Bunkyo, Tokyo 113-0033, Japan

K. Yoshikawa Faculty of Life and Medical Sciences Doshisha University Kyoto 610-0394, Japan

Supporting information for this article is available on the WWW under https://doi.org/10.1002/cbic.202500665



(t = 14 s).

solution without lecithin. Two neighboring DEX droplets move directly toward each other until they make contact, which we denote as the 0-second mark. After a brief period of contact, the droplets begin to merge at 14 s, eventually forming a single droplet by 19 s. To analyze the processes of approach, contact, and coalescence, we analyzed spatial intensity profiles. During the approaching process, two distinct peaks corresponding to the individual droplets are observed (Figure 1c; at $140-170\,\mu m$ of t=-37 s). At the moment of contact (0 s), these central peaks overlap, merging into a single peak (t=0 s). During coalescence, the two droplets begin merging and the central peak disappears

We observe and analyze this coalescence process of DEX droplets for with or without lecithin samples. We evaluate the rate of this process by dividing it into two sequential dynamic stages: approaching migration speed, which reflects the strength of attractive interactions and influences the collision frequency of the droplets, and the coalescence rate that occurs upon contact.

To analyze the effect of lecithin on the droplet's stability, we added lecithin to the PEG/DEX system at various concentrations, $C_{\rm L}$, ranging from 0 to 2.0 mg mL $^{-1}$ (see Section 4.2 for the experimental details). We evaluate migration speed $V_{\rm a}$ from droplet pairs (droplet's R is ranged from 30 to 175 µm) separated by \approx 20 µm or more, which were randomly selected. As shown in movie S1, such pairs typically approached each other directly. Two representative plots of d(t) versus time t before contact for $C_{\rm L}=0$ mg mL $^{-1}$ are shown in Figure S1, Supporting Information, demonstrating a linear relationship (Figure S1, Supporting Information). Therefore, we obtain the velocity $V_{\rm a}$ [µm/s] as the slope between the initial and contact points (d=0 mm). The relative migration speed $V_{\rm a}\equiv d/\Delta t$ is also defined as where d is the initial surface-to-surface distance between the two droplets, and Δt is the lag time before contact.

Figure 2a displays the average values of V_a calculated from 5 pairs of droplets at each C_L . Under fixed C_L conditions, we have found no significant correlation between V_a and R of the droplet pairs (Figure S2, Supporting Information), even for R values above and below the depth of the observation chamber, $\approx 90 \, \mu m$. Although the measured migration speeds V_a show some variability, they remain nearly constant ($\approx 0.4 \, \mu m \, s^{-1}$) at lecithin concentrations C_L below 0.1 mg mL⁻¹, indicating no notable effect of lecithin at these levels. However, above 0.1 mg mL⁻¹, V_a experiences a sharp decline and then stabilizes at a lower value, indicating that droplets take considerably longer to come into contact.

While higher lecithin concentrations could increase the solution viscosity, thereby reducing V_a , the measured viscosity of the lecithin-containing solution (1.2 mPa s at $C_L = 4.0$ mg mL⁻¹) (see Section 4.6 for Experimental Section) is only slightly higher than that of pure water (1.0 mPa s). Since migration speed is expected to be inversely proportional to viscosity, assuming other properties remain constant, the observed decrease to $\approx 25\%$ in V_a at concentrations above 0.1 mg mL⁻¹ cannot be attributed solely to viscosity changes. This drop is likely influenced by lecithin's effect on inter-droplet interactions. These interactions may

presented in their study indicate potential applications as semipermeable membranous microcompartments, contributing to advancements in synthetic biology and biochemical reaction control. In a related study, Zhang et al., reported that the adsorption of SUVs containing anionic phosphatidylglycerol and PEGylated phospholipids effectively stabilized DEX droplets in PEG solution. The movement of DEX droplets was attributed to the Marangoni flow generated by a PEG concentration gradient within the surrounding medium.[19,23] It was proposed that this gradient experienced weakening due to the partial coverage of the droplets by SUVs, resulting in altered droplet motility. Consequently, applying lipid coverage to ATPS droplets may improve their static stability, dynamic behavior, and transport mechanisms. Most prior studies using lipids have assessed droplet stability by monitoring changes in average droplet size over time. However, overall droplet growth is governed by two distinct processes: 1) droplet migration, driven not only by diffusion but also by attractive inter-droplet interactions that increase collision frequency and 2) the coalescence after droplet contact or collisions. To the best of our knowledge, these two processes have not been independently quantified.

In this study, we address this gap by separately evaluating droplet migration and coalescence for DEX droplets in a PEG solution under the presence of lipids. This study examines the coating effect of soybean lecithin; a biologically relevant material widely used in a variety of applications. Soybean lecithin primarily consists of zwitterionic phosphatidylcholine (PC), phosphatidylethanolamine (PE), and anionic phosphatidylinositol (PI), although the exact composition varies depending on the purification process.[24] It has been proposed that soybean lecithin can stabilize ATPS droplets by simply dissolving it in water with a vortex.^[6] Additionally, the soybean lecithin used here is a mixture of diverse phospholipids, similar to the composition of SUVs, which have been previously reported to stabilize ATPS droplets. [8,19,23] The lipids found in living cell membranes are also diverse, and this complex composition is expected to impart properties closer to those of living organisms. Notably, we observe that lecithin significantly slows both migration and coalescence, but only above its critical micelle concentration (CMC), with coalescence being particularly strongly inhibited. These findings highlight a simple yet effective strategy for stabilizing ATPS droplets and provide new mechanistic insight into how lipid adsorption controls droplet dynamics.

2. Results and Discussion

Using DEX droplets in a PEG solution (5 wt% DEX and 5 wt% PEG mixture; see the Experimental Section 4.1 for the details), we investigated a strategy to enable ATPS droplets to exist more stably without colliding or coalescing. All experiments are performed at ≈ 24 °C. To simplify the analysis, we used a water depth setup of 90 μ m and investigated the behavior of DEX droplets with diameters from 60 to 350 μ m (**Figure 1**a; see also Experimental Section 4.3). Figure 1b shows the approaching migration and coalescence process of DEX droplets in a PEG

oaded from https://chemistry-europe.onlinelibrary.wiley.com/doi/10.1002/cbic.202500665, Wiley Online Library on [08/11/2025]. See the Terms and Conditions (https://onlinelibrary.wiley.com/terms-and-conditions) on Wiley Online Library for rules of use; OA articles are governed by the applicable Creative Commons Licensen

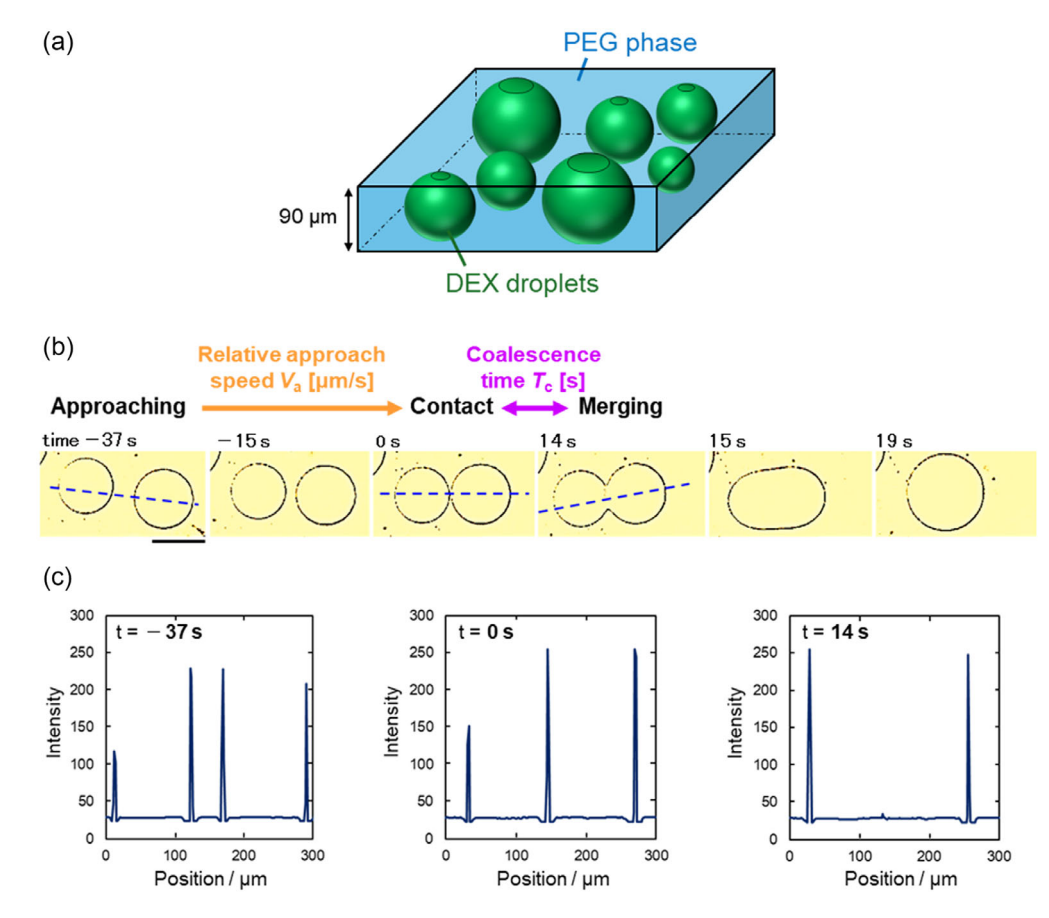


Figure 1. Spontaneous approach and coalescence of DEX droplets in a PEG solution. a) Schematic representation of the 90 µm depth setup used to observe DEX droplets (shown in green) in a PEG solution (shown in blue). b) Time-lapse microscopic images illustrate the migration and coalescence of DEX droplets in the PEG/DEX system (5 wt% DEX: 5 wt% PEG) without the addition of lecithin. The neighboring droplets with radius R (50-60 µm) move linearly toward each other until they make contact. The time is set to 0 s at the moment of contact. After a brief delay, they begin to merge at 14 s and fully coalesce into a single droplet by 19 s. Scale bar: $100 \, \mu m. c$) Intensity profiles measured along the dashed line depicted in panel (b), recorded at $t = -37 \, s$ (approach), 0 s (contact), and 14 s (merging).

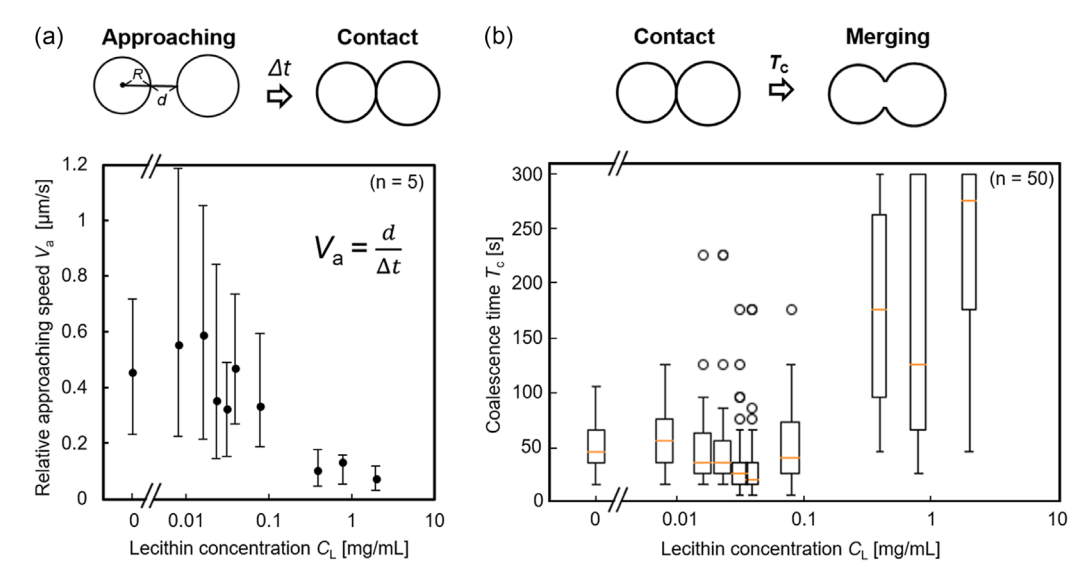


Figure 2. Approaching speed and coalescence time of DEX droplets. a) Top: Schematic illustration of the calculation of the relative approaching speed V_a between two droplets, with the droplet radius R_i , distance between approaching droplets d_i , and the lag time before contact Δt . Bottom: Plot of migration speed V_a (= $d/\Delta t$) as a function of lecithin concentration C_1 . Error bars represent the minimum and maximum measurements (n = 5). b) Top: Schematic diagram illustrating the coalescence time T_c from the point of contact until the onset of merging. Bottom: box-and-whisker plot of T_c versus C_L (n = 50). Outliers are indicated by open circles.

involve attractive forces due to the nonequilibrium distribution of polymers around the droplets, although this remains uncertain.^[25–27]

After the droplets made contact, the initiation time for coalescence T_c was measured. T_c was defined as the duration from the moment of contact (Figure 1b,c, t = 0 s) to the onset of surface rupture leading to merging (Figure 1b,c, $t = 14 \, \text{s}$). Under fixed C_1 conditions, T_c was measured for 50 droplet pairs, which allowed us to generate histograms. The results are summarized in a box-and-whisker plot (Figure 2b), with the corresponding histograms displayed in Figure S3, Supporting Information. T_c remained nearly constant at C_L below 0.1 mg mL⁻¹, indicating no notable effect of lecithin at these levels. It increased sharply above 0.1 mg mL⁻¹ and eventually stabilized. This suggests that the impact of lecithin concentration on coalescence dynamics changes significantly around $C_L \approx 0.1 \text{ mg mL}^{-1}$. Overall, the results shown in Figure 2a,b indicate that lecithin slows both the approach of droplets and their coalescence, with this effect becoming significant at lecithin concentrations above 0.1 mg mL^{-1} .

The effect of lecithin on droplet growth was assessed by monitoring the overall growth of individual droplets over time. **Figure 3** shows the change in radius of randomly selected droplets undergoing fusion with surrounding over a period of 1 h. The initial and final radii are defined as R_0 and R_{60} , respectively. For each droplet, the ratio R_{60}/R_0 was calculated, and the average was obtained from five droplets randomly selected at each $C_{\rm L}$. In cases where two selected droplets fuzed during the observation period, the same R_{60} value was assigned to both, but different R_0 values were used, resulting in two distinct R_{60}/R_0 values.

At C_L levels below ≈ 0.1 mg mL⁻¹, the droplet radius increased significantly, reaching 3–7 times its initial size, R_0 . In contrast, growth was markedly suppressed at higher lecithin concentrations ($C_L > \approx 0.1$ mg mL⁻¹). This concentration range aligns closely with the levels at which significant changes were observed in both T_c and V_a (see Figure 2), further supporting the conclusion that lecithin significantly inhibits droplet migration and coalescence at $C_L > 0.1$ mg mL⁻¹, thereby improving droplet stability. Although a peak appears at a concentration slightly above 0.02 mg mL⁻¹, this observation may have been influenced by local concentration fluctuations due to the extremely low overall concentration.

Figure 4 shows fluorescence microscopy images of ATPS droplets at varying lecithin concentrations. At $C_L = 0 \text{ mg mL}^{-1}$, the fluorescence signal was very weak compared to lecithin-containing samples. Therefore, the detector sensitivity was increased only for this condition to improve visibility. At this $C_L = 0 \text{ mg mL}^{-1}$ condition, the fluorescent probe, Rhodamine 6G, was primarily observed in the PEG-rich phase, consistent with its preferential partitioning into the less hydrophilic environment. At $C_L = 0.01 \text{ mg mL}^{-1}$, weak fluorescent speckles began to appear along the droplet boundaries, even without increasing detector sensitivity. Since Rhodamine 6G accumulates in lecithin-rich regions, this result suggests that lecithin molecules are slightly

adsorbed at the surface of the DEX droplets. This is supported by the comparison between fluorescence and merged bright-field images. As the lecithin concentration increased, the fluorescence intensity became progressively more concentrated at the droplet interfaces ($C_L = 0.04 - 0.08 \text{ mg mL}^{-1}$). Notably, above $C_L \approx 0.12 \text{ mg mL}^{-1}$, the fluorescence became sharply localized at the droplet surfaces. This transition closely corresponds to the lecithin concentration of 0.1 mg mL⁻¹ in which droplet growth and coalescence were significantly suppressed (Figure 2 and 3).

The results indicate that when lecithin is present at concentrations above 0.1 mg mL⁻¹, it can completely cover the DEX droplets, improving the stability of the DEX droplets. To understand this critical concentration of 0.1 mg mL⁻¹, we investigated the CMC of lecithin. The CMC was determined by surface tension measurements (see Section 4.5 for experimental details) and found to be $\approx 0.078 \,\mathrm{mg}\,\mathrm{mL}^{-1}$ (Figure S4, Supporting Information). This value is consistent with the typical CMC of crude soybean-derived lecithin in aqueous solution (0.291 mg mL⁻¹) and that of hydroxylated soybean lecithin (0.112 mg mL⁻¹).^[28] These results strongly suggest that at concentrations above 0.1 mg mL⁻¹, lecithin molecules form micelles or aggregates in solution, which efficiently adsorb and coat the droplet surface. Soybean lecithin contains not only phospholipids but also triglycerides, fatty acids, glycolipids, and sterols, which are believed to increase the CMC compared to pure phospholipids.[29,30]

Figure 2a suggests that the adsorption layer of lecithin formed at $C_1 > 0.1 \text{ mg mL}^{-1}$ also reduces the attractive interactions between DEX droplets. These inter-droplet interactions are typically governed by surface forces such as van der Waals attraction and overlapping electrical double layers and may be influenced by other nonequilibrium effects.^[12,13,31,32] Our results indicate that the presence of micelles or their aggregates of lecithin on the droplet surface weakens these attractive forces. When lecithin forms a concentrated surface layer, solvent molecules are osmotically driven to enter this region. However, the strong affinity between micelles (or aggregates) and the droplet surface resists such solvent intrusion. When two droplets approach each other, their respective surface-layers overlap, resulting in an increased local concentration of lecithin in the contact region. This leads to elevated osmotic pressure that eventually overcomes the interfacial affinity, allowing solvent molecules to invade the overlapping layer, thereby weaken the net attractive interaction between droplets. Such an effect only occurs when micelles or aggregates are present, which explains the sharp reduction in the migration speed V_a observed at $C_1 > 0.1 \text{ mg mL}^{-1}$.

Previous studies on the interfacial adsorption behavior of phospholipids have shown that SUVs of phospholipids can stabilize droplets by adsorbing onto their surfaces. [8,12,14,20,22] These studies typically assume that the vesicles are well-dispersed, having been prepared through methods like sonication or centrifugation. However, in our study, we did not use sonication or centrifugation during the preparation of lecithin.

ded from https://chemistry-europe.onlinelibrary.wiley.com/doi/10.1002/cbic.202500665, Wiley Online Library on [08/11/2025]. See the Terms

and-conditions) on Wiley Online Library for rules of use; OA articles are governed by the applicable Creative Commons License

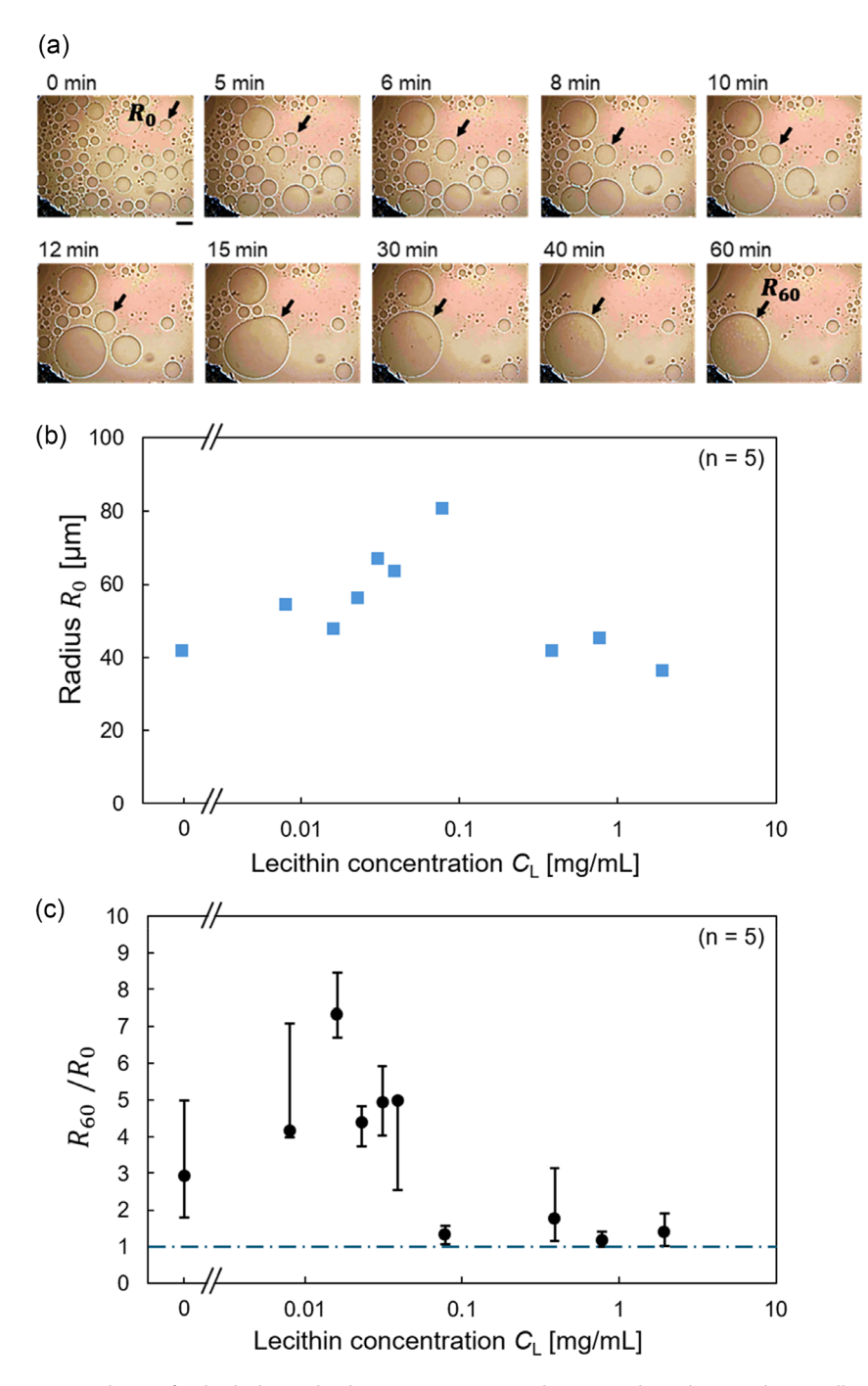


Figure 3. Changes in the average radius R of individual DEX droplets over time. a) Time-lapse snapshots showing the overall growth of a single droplet. Scale bar: $100 \, \mu m$. b) The initial average radius (R_0) of droplets at each lecithin concentration immediately after the addition of the lecithin (n = 5). c) Evolution of the average droplet radius over 60 min (R_{60}) normalized by the initial radius, R_{60}/R_0 . Error bars represent the minimum and maximum measurements (n = 5).

This suggests that the observed stabilizing effect may be attributed to the spontaneous formation of micelles or aggregates, rather than SUVs. The presence of micellar or aggregated layers at the droplet interface likely acts as a protective barrier, thereby reducing coalescence and slowing the overall growth of the droplets.

The adsorption of lipids onto the ATPS droplet surface, as well as the lipid structure formed on the droplet, is expected to be influenced by several factors, including the composition of the lipids, the method of lipid dissolution in the solvent, dissolved ions and substance of aqueous phase, and the temperature. Indeed, previous in vitro studies of phospholipid bilayers have reported that complex lipid mixtures such as soybean lecithin more effectively reproduce the functional properties of membrane channel proteins compared to bilayers made from pure lipid components.[24,33] A comprehensive

aded from https://chemistry-europe.onlinelibrary.wiley.com/doi/10.1002/cbic.202500665, Wiley Online Library on [08/11/2025]. See the Terms and Conditions (https://onlinelibrary.wiley.com/terms-and-conditions) on Wiley Online Library for rules of use; OA articles are governed by the applicable Creative Commons. Licenses, and Conditions (https://onlinelibrary.wiley.com/terms-and-conditions) on Wiley Online Library for rules of use; OA articles are governed by the applicable Creative Commons. Licenses, and Conditions (https://onlinelibrary.wiley.com/terms-and-conditions) on Wiley Online Library for rules of use; OA articles are governed by the applicable Creative Commons. Licenses, and Conditions (https://onlinelibrary.wiley.com/terms-and-conditions) on Wiley Online Library for rules of use; OA articles are governed by the applicable Creative Commons. Licenses, and Conditions (https://onlinelibrary.wiley.com/terms-and-conditions) on Wiley Online Library for rules of use; OA articles are governed by the applicable Creative Commons. Licenses, and Conditions (https://onlinelibrary.wiley.com/terms-and-conditions) on Wiley Online Library for rules of use; OA articles are governed by the applicable Creative Commons. Licenses, and Conditions (https://onlinelibrary.wiley.com/terms-and-conditions) on Wiley Online Library for the applicable Creative Commons. Licenses, and the ap

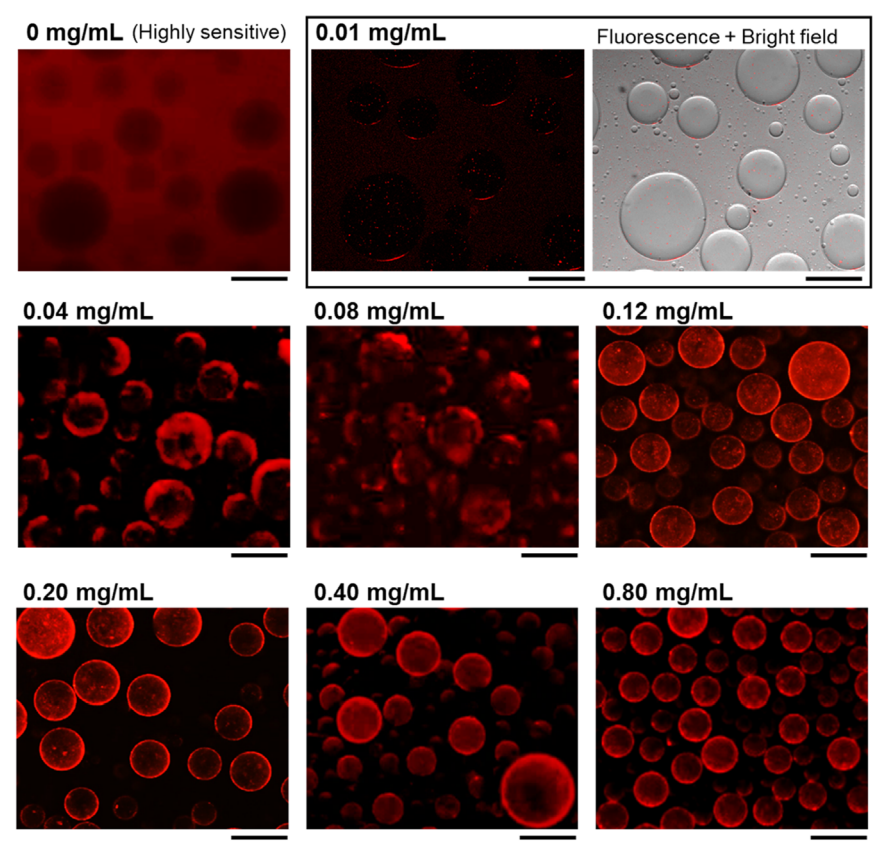


Figure 4. Fluorescence microscopy images of DEX droplets, both with or without lecithin. In the system with added lecithin, the fluorescent dye Rhodamine 6G preferentially localizes in lecithin-rich regions. At $C_L = 0.04$ and 0.08 mg mL⁻¹. Fluorescence localization is observed at a portion of the droplets; however, at $C_L = 0.12$ mg mL⁻¹ and higher, fluorescence covers the entire droplet surface. The right panel ($C_L = 0.01$ mg mL⁻¹) shows a merged fluorescence and bright-field image. Scale bars: $100 \, \mu m$.

understanding of these determinants presents a significant challenge for future research.

3. Conclusion

Lecithin enhances the stability of aqueous two-phase droplets through two distinct mechanisms. First, micelle formation reduces droplet–droplet attraction, slowing their mutual approach. More importantly, the adsorption of lecithin micelles or aggregates at the droplet interface forms a protective layer that effectively prevents coalescence. This interfacial barrier plays a dominant role in suppressing droplet growth and maintaining long-term droplet stability.

4. Experimental Section

Preparation of DEX Droplets in a PEG Solution

Polyethylene glycol (PEG, average molecular weight [MW] = 6000) and dextran (DEX, MW = 200 000) were purchased from Fujifilm Wako Pure Chemical Industries (Osaka, Japan). A polymer mixture containing 5 wt% PEG and 5 wt% DEX, corresponding to a phase-separated state near the binodal line of the ATPS, [34] was

prepared by dissolving the polymers in fully deionized water (ELGA LabWater, Purelab Flex 3; $40\,\mathrm{mL}$).

Preparation of DEX Droplets with Lecithin

Lecithin powder (Product No. 20335-52; Soybean Lecithin \geq 60%, Practical Grade CP [Reagent]; Nacalai Tesque Inc., Kyoto, Japan) and a fluorescent dye (Rhodamine 6G; excitation wavelength: 525 nm; emission wavelength: 548 nm; Fujifilm Wako Pure Chemical Industries, Osaka, Japan) were used. The lecithin powder was dissolved in deionized water by mixing with a vortex mixer for 5 min, without sonication or centrifugation, and then allowed to stand at \approx 24 °C for several days. Subsequently, after brief mixing with a vortex mixer (3 s), the lecithin solution was mixed with the PEG/DEX solution to achieve final lecithin concentrations ranging from 0 to 2.0 mg mL $^{-1}$.

Microscopic Observation of DEX Droplets

For microscopy, double-sided tape with a punched hole (90 μ m depth; 1.5 mm diameter) was placed on a glass slide. Immediately after mixing the prepared solution with a vortex mixer for 3 s, it was injected into the hole and covered with a cover glass. Images of bright fields and fluorescence were acquired using a phase-contrast microscope (Olympus IX71; Olympus Co., Tokyo, Japan) with a complementary metal oxide semiconductor (CMOS) digital camera (DP74; Olympus Co., Tokyo, Japan). All experiments are performed at \approx 24 °C.



Analysis of Droplet Movement

We selected DEX droplets with diameters from 60 to 350 μ m for the analysis of droplet movement. Videos were recorded at 30 frames per second, providing a time resolution of 0.033 s. The coordinates of each droplet center and the area of each droplet were obtained using image processing software (ImageJ). The droplet radius was defined as that of a circle with an area equal to the droplet's cross-sectional area observed in the microscope images. The distance d was calculated as the center-to-center distance between two droplets minus the sum of their radii. In each video, five pairs of droplets showing linear approach, collision, and contact were selected.

Surface Tension Measurements

The surface tension of the lecithin-containing aqueous solution was measured by the pendant drop measurements (the captured droplet images using the ds/de method) using an optical tensiometer (Attension Theta (Biolin Scientific)) at $\approx\!24\,^{\circ}\text{C}$. The densities were measured by pycnometer.

Viscosity Measurements

The viscosity of lecithin-containing water was measured by the cone and plate viscometer (ViscoQC 300 L; Anton Paar.).

Acknowledgements

This research was supported by the Japan Society for the Promotion of Science (JSPS) KAKENHI grant numbers 23KJ2081, 25KJ0083 (M.S.), JSPS 24H02287, 23K22459 (JST), grant numbers FOREST, JPMJFR213Y, CREST, JPMJCR22E1 (M.Y.), 22K03560 (A.S.). Fusion Oriented Research for disruptive Science and Technology (JPMJFR213Y). Core Research for Evolutional Science and Technology (JPMJCR22E1).

Conflict of Interest

The authors declare no conflict of interest.

Data Availability Statement

The data that support the findings of this study are available from the corresponding author upon reasonable request.

Keywords: aqueous two-phase systems \cdot critical micelle concentration \cdot lecithin \cdot liquid–liquid phase separation \cdot phospholipids membranes

- P.-Å. Albertsson, in Advances in Protein Chemistry (Eds: C. B. Anfinsen, J. T. Edsall, F. M. Richards), vol. 24, Academic Press 1970, pp. 309–341.
- [2] N. Nakatani, H. Sakuta, M. Hayashi, S. Tanaka, K. Takiguchi, K. Tsumoto, K. Yoshikawa, ChemBioChem 2018, 19, 1370.
- [3] S. Deshpande, F. Brandenburg, A. Lau, M. G. F. Last, W. K. Spoelstra, L. Reese, S. Wunnava, M. Dogterom, C. Dekker, *Nat. Commun.* 2019, 10, 1800.
- [4] J. W. Szostak, D. P. Bartel, P. L. Luisi, Nature 2001, 409, 387.
- [5] M. Zhu, Z. Li, J. Li, Y. Lin, H. Chen, X. Qiao, X. Wang, X. Liu, X. Huang, *Nat. Commun.* 2025, 16, 1783.
- [6] H. Sakuta, F. Fujita, T. Hamada, M. Hayashi, K. Takiguchi, K. Tsumoto, K. Yoshikawa. ChemBioChem 2020, 21, 3323.
- [7] Y. Minagawa, M. Yabuta, M. Su'etsugu, H. Noji, Nat. Commun. 2025, 16, 1522.
- [8] A. T. Rowland, C. D. Keating, Soft Matter 2021, 17, 3688.
- [9] B. T. Nguyen, T. Nicolai, L. Benyahia, Langmuir 2013, 29, 10658.
- [10] D. M. Buzza, P. D. Fletcher, T. K. Georgiou, N. Ghasdian, *Langmuir* 2013, 29, 14804.
- [11] Y. Zhang, Z. Zhi, T. Jiang, J. Zhang, Z. Wang, S. Wang, J. Control Release 2010, 145, 257.
- [12] D. C. Dewey, C. A. Strulson, D. N. Cacace, P. C. Bevilacqua, C. D. Keating, Nat. Commun. 2014, 5, 4670.
- [13] Y. Wang, Y. Zhao, L. Sun, A. A. Mehrizi, S. Lin, J. Guo, L. Chen, *Langmuir* 2022, 38, 3860.
- [14] C. Fick, Z. Khan, S. Srivastava, Mater. Adv. 2023, 4, 4665-4678.
- [15] N. Coudon, L. Navailles, F. Nallet, I. Ly, A. Bentaleb, J.-P. Chapel, L. Béven, J.-P. Douliez, N. Martin, J. Colloid Interface Sci. 2022, 617, 257.
- [16] M. Pavlovic, A. Plucinski, L. Zeininger, B. V. K. J. Schmidt, Chem. Commun. 2020, 56, 6814.
- [17] H. Seo, C. Nam, E. Kim, J. Son, H. Lee, ACS Appl. Mater. Interfaces 2020, 12, 55467.
- [18] S. Tan, Y. Ai, X. Yin, Z. Xue, X. Fang, Q. Liang, X. Gong, X. Dai, Adv. Funct. Mater. 2023, 33, 2305071.
- [19] S. Zhang, C. Contini, J. W. Hindley, G. Bolognesi, Y. Elani, O. Ces, *Nat. Commun.* 2021, 12, 1673.
- [20] F. P. Cakmak, A. M. Marianelli, C. D. Keating, Langmuir 2021, 37, 10366.
- [21] C. D. Keating, Acc. Chem. Res. 2012, 45, 2114.
- [22] T. Lu, S. Javed, C. Bonfio, E. Spruijt, Small Methods 2023, 7, 2300294.
- [23] T. Furuki, H. Sakuta, N. Yanagisawa, S. Tabuchi, A. Kamo, D. S. Shimamoto, M. Yanagisawa, ACS Appl. Mater. Interfaces 2024, 16, 43016.
- [24] Y. Wu, T. Wang, J. Amer. Oil Chem. Soc. 2003, 80, 319.
- [25] T. Ban, T. Yamada, A. Aoyama, Y. Takagi, Y. Okano, Soft Matter 2012, 8, 3908.
- [26] T. Ban, A. Aoyama, T. Matsumoto, Chem. Lett. 2010, 39, 1294.
- [27] R. Shimizu, H. Tanaka, Nat. Commun. 2015, 6, 7407.
- [28] P. P. Chiplunkar, A. P. Pratap, J. Oleo Sci. 2017, 66, 1101.
- [29] W. Johnson, W. F. Bergfeld, D. V. Belsito, R. A. Hill, C. D. Klaassen, D. C. Liebler, J. G. Marks, R. C. Shank, T. J. Slaga, P. W. Snyder, L. J. Gill, B. Heldreth, Int. J. Toxicol. 2020, 39, 55.
- [30] J. S. U. Tabaniag, M. Q. D. Abad, C. J. R. Morcelos, G. V. B. Geraldino, J. L. M. Alvarado, E. C. R. Lopez, J. Eng. Appl. Sci. 2023, 70, 154.
- [31] F. Dumas, J.-P. Benoit, P. Saulnier, E. Roger, J. Colloid Interface Sci. 2021, 599, 642.
- [32] M. Shono, F. Fujita, K. Yoshikawa, A. Shioi, Chem. Lett. 2023, 52, 794.
- [33] L. Rydhag, I. Wilton, J. Amer. Oil Chem. Soc. 1981, 58, 830.
- [34] K. Tsumoto, M. Arai, N. Nakatani, S. Watanabe, K. Yoshikawa, *Life* 2015, 5, 459.

Manuscript received: September 1, 2025 Revised manuscript received: October 22, 2025 Version of record online: